# BEDT-TTF Salts with α-Keggin Polyoxometallates: Electrical, Magnetic, and Optical Properties of $(BEDT\text{-}TTF)_8[PMo_{12}O_{40}]$ and $(BEDT\text{-}TTF)_8[SiW_{12}O_{40}]$ and X-ray Crystal Structure of $(BEDT\text{-}TTF)_8[PMo_{12}O_{40}]\cdot\{(CH_3CN\cdot H_2O)_2\}$

Carlo Bellitto,* Mario Bonamico,* Vincenzo Fares, Fulvio Federici, and Guido Righini

*Istituto di Chimica dei Materiali del C.N.R., Area della Ricerca di Roma C.P. 10, Via Salaria km.29.5, I-00016 Monterotondo Staz., Roma, Italy*

Mohamedally Kurmoo* and Peter Day

*The Royal Institution of Great Britain, 21 Albemarle Street, London, WX1 4BS U.K.*

*Received January 3, 1995. Revised Manuscript Received May 16, 1995*[⊗]

We report the electrical, magnetic, and optical properties of two isomorphous salts of BEDT-TTF, bis(ethylenedithio)tetrathiafulvalene, with α-Keggin anions, viz., $(BEDT\text{-}TTF)_8[PMo_{12}O_{40}]\cdot\{(CH_3CN\cdot H_2O)_2\}$ and $(BEDT\text{-}TTF)_8[SiW_{12}O_{40}]$. The former crystallizes in the monoclinic space group $I2$ with $a = 14.086(6)$, $b = 43.26(1)$, $c = 14.062(6)$ Å, $\beta = 107.84(4)°$, $Z = 2$. The structure consists of alternate layers of BEDT-TTF, organized as a pseudo-α-phase, and of the α-Keggin inorganic anions and solvents of crystallization, along the $b$ axis. For the $PMo_{12}O_{40}$ salt $\sigma_{RT} = 10^{-1}$ S cm$^{-1}$, $E_A = 0.088$ eV for $T < 150$ K and 0.177 eV for $T > 200$ K and for the $SiW_{12}O_{40}$ salt $\sigma_{RT} = 0.4$ S cm$^{-1}$ and $E_A = 0.098$ eV. The conductivity anisotropy is 0.1:0.05:0.009 and 0.4:0.13, respectively. The magnetic properties are the sum of those of the BEDT-TTF layers, which is a combination of a uniform 1D linear chain antiferromagnet ($\alpha = 1$) with $J/k_B = -27$ K for $SiW_{12}O_{40}$ and $-43$ K $PMo_{12}O_{40}$ and a dimerized chain antiferromagnet ($\alpha = 0$) with $\Delta/k_B = -96.5$ and $-145$ K, respectively, and of the anions which is diamagnetic for the $SiW_{12}O_{40}$ salt and Curie paramagnetic ($S = {}^1/_2$) for $PMo_{12}O_{40}$. The EPR of the $SiW_{12}O_{40}$ salt is dominated by the resonance from the BEDT-TTF moiety. The $PMo_{12}O_{40}$ salt shows one resonance, which comprises a combination of both the anion and the BEDT-TTF radical, above 150 K. As the temperature of the sample is lowered, it splits into two components; the one at lower $g$ value grows at the expense of the other. From the temperature dependence of the intensities, we estimate an energy difference of 1.2(8) K. Both components show weak fine structures that originate from $^{95}$Mo and $^{97}$Mo (each with $I = {}^5/_2$). The optical data show a polarized intraband transition at ~2000 cm$^{-1}$ (0.25 eV) consistent with the electrical measurements. The two compounds presented here are on the borderline of the Mott–Hubbard transition.

## Introduction

Radical cation salts of the donor BEDT-TTF [bis(ethylenedithio)tetrathiafulvalene] and related oxo- and seleno-substituted molecules, BEDO-TTF [bis(ethylenedioxo)tetrathiafulvalene] and BEDT-TSF [bis(ethylenedithio)tetraselenofulvalene], respectively, have attracted much interest since the discovery of superconductivity in organic materials.[1–3] These compounds usually crystallize in two-dimensional layers of the conducting donors with considerable interactions between the chalcogen atoms, leading to band formation; the conducting layers alternate with the insulating layers of the anion. A large number of BEDT-TTF radical ion salts with small closed-shell anions have been studied extensively. Over 30 have been found to be superconducting: the highest critical temperature being 13 K.[2] For the two structural classes of organic superconductors, the $\beta$ and $\kappa$ phases, increasing the volume of the anion results in an increase of the critical temperature.[4] Conducting salts have been observed with cluster anions of as many as 24 atoms but only when the 2D layer structure is conserved, but no superconducting salt has been isolated.[5–6] As part of our interest on the effect of the size, shape, and magnetic moment of the anion on the crystal structure and on the physical properties of the material,[7] we consider the heteropolyanion clusters with the α-Keggin structure, $[XO_4Mo_{12}O_{36}]^{n-}$,[8] to be good candidates to use as anions with BEDT-TTF. The

[⊗] Abstract published in *Advance ACS Abstracts,* June 15, 1995.

(1) See, for example: *Proceedings of the International Conference of Synthetic Metals. Synth. Met.* **1989**, *27*; **1991**, *41–43*; **1993**, *55–57*.

(2) Williams, J. M.; Ferraro, J. R.; Thorn, R. J.; Carlson, K. D.; Geiser, U.; Wang, H. H.; Kini, A. M.; Whangbo, M. H. *Organic Superconductors: (including fullerene)*; Prentice Hall: Englewood Cliffs, NJ, 1992.

(3) Ishiguro, T.; Yamaji, K. *Organic Superconductors*; Springer-Verlag: Berlin, 1990; Vol. 88.

(4) Williams, J. M.; Schultz, A. J.; Geiser, U.; Carlson, K. D.; Kini, A. M.; Kwock, W. K.; Whangbo, M. H.; Schirber, J. E. *Science* **1991**, *252*, 1501.

(5) Penicaud, A.; Boubekeur, K.; Batail, P.; Canadell, E.; Auban-Senzier, P.; Jérome, D. *J. Am. Chem. Soc.* **1993**, *115*, 4101.

0897-4756/95/2807-1475$09.00/0 

cluster can be easily reduced to a paramagnetic class IIIA mixed-valence[9] cluster $[PMo_{12}O_{40}]^{4-}$, which may give an insight of the interaction of localized moments on the anion and the electron gas in the organic donors, and to the diamagnetic *two*-electron-reduced cluster $[PMo_{12}O_{40}]^{5-}$. Electrocrystallization of BEDT-TTF in the presence of $[PMo_{12}O_{40}]^{3-}$ produces three phases, two characterized with the formulas $(BEDT\text{-}TTF)_8[PMo_{12}O_{40}]\cdot\{(CH_3CN\cdot H_2O)_2\}$ and $(BEDT\text{-}TTF)_6[PMo_{12}O_{40}]\cdot\{(CH_3CN)_4\cdot(H_2O)_3\}$[10] and a third phase under study. With the $[SiW_{12}O_{40}]^{4-}$ anion, only one phase has so far been characterized, and it is not solvated.[11]

This paper describes the synthesis, crystal structure, and the electrical, magnetic, and optical properties of $(BEDT\text{-}TTF)_8[PMo_{12}O_{40}]\cdot\{(CH_3CN\cdot H_2O)_2\}$ and the physical properties of $(BEDT\text{-}TTF)_8[SiW_{12}O_{40}]$ for comparison. Brief communications of the synthesis and magnetic properties have been presented earlier.[6d,10]

## Experimental Section

**Synthesis.** Elemental analyses were performed by Malissa & Reuter Mikroanalytische Laboratorium, Elbach, Germany, and by Laboratorio di Microanalisi del C.N.R., Area della Ricerca di Roma. All solvents were reagent grade, freshly distilled, and degassed with argon or nitrogen prior to use.

**Starting Materials.** BEDT-TTF, $(NBu_4)_3[PMo_{12}O_{40}]$, $(NEt_4)_3[PMo_{12}O_{40}]$, and $(NEt_4)_4[SiW_{12}O_{40}]$ were prepared according to the literature.[12,13]

**$(NBu_4)_4[PMo_{12}O_{40}]$.** To obtain high purity, we have prepared this compound electrochemically. An oxygen-free acetonitrile solution (70 mL) of $(NBu_4)_3[PMo_{12}O_{40}]$ (0.526 g, $2.06 \times 10^{-4}$ mol) were electrolyzed at a constant voltage of −0.4 V vs Ag/AgCl electrode in the presence of an excess of $(NBu_4)[PF_6]$. The electrolysis was stopped when the number of coulombs consumed were those corresponding to 90% of that expected for the quantity of the starting materials, 18 C. The volume of the resulting dark green solution was reduced to 30 mL. On cooling, dark green prismatic crystals were obtained.

**Charge-Transfer Salts of BEDT-TTF with $PMo_{12}O_{40}$ and $SiW_{12}O_{40}$.** Black shiny hexagonal plates or square cross-sectioned needles were obtained by the electrocrystallization method as described previously.[6d,11] The stoichiometry (ratio of S to Mo) of the 8:1 salt was determined by elemental analysis and by X-ray photoelectron spectroscopy (vide infra). Better quality crystals of $(BEDT\text{-}TTF)_8[PMo_{12}O_{40}]\cdot\{(CH_3CN\cdot H_2O)_2\}$ were obtained in the presence of 18crown6. All measurements reported here were made on these crystals.

## Physical Measurements

**Cyclic Voltammetry.** Electrochemical measurements were performed with an AMEL electrochemistry system with two platinum and one Ag/AgCl electrodes in dried and deoxygenated acetonitrile solutions. Tetrabutylammonium hexafluorophosphate or tetrabutylammonium tetrafluoroborate salts was used as supporting electrolytes.

**Thermogravimetric Analysis.** The weight loss from two batches of $(BEDT\text{-}TTF)_8[PMo_{12}O_{40}]\cdot\{(CH_3CN\cdot H_2O)_2\}$ (~4.5 mg each) was measured in dry nitrogen on a Stanton-Redcroft STA-781 thermoanalyzer. Between 35 and 180 °C 2.2% is lost, close to that expected for two water and two acetonitrile molecules per formula unit.

**X-ray Crystal Structure Analysis.** A summary of the crystallographic data and structure determination for $(BEDT\text{-}TTF)_8[PMo_{12}O_{40}]\cdot\{(CH_3CN\cdot H_2O)_2\}$ is provided in Table 1. A well-grown crystal was used for data collection. The data were corrected for Lorentz and polarization factors. The choice of the nonprimitive *I*2 space group was suggested by the isomorphism with the crystals of $(BEDT\text{-}TTF)_8[SiW_{12}O_{40}]$.[11] $(BEDT\text{-}TTF)_8[PMo_{12}O_{40}]\cdot\{(CH_3CN\cdot H_2O)_2\}$ is found to have an organic layer structure similar to that in the silicotungstate. The difference is a 2-fold positional disorder in the orientation of the radical cations and the presence in the unit cell of two acetonitrile molecules and two of water. Each BEDT-TTF molecule occupies two positions in such a way that the two orientations form a dihedral angle of ~45° when viewed along the central C=C bond. One of the orientations is similar to that observed in the silicotungstate compound, and it is present in this structure with an occupation factor of 1/3. The central $[PO_4]$ group of the cluster is also disordered, with the phosphorus atom surrounded by a distorted cube of oxygens atoms, formed by the overlap of the two $O_4$ tetrahedra having an occupancy factor of 2/3 and 1/3

**Table 1. Structure Determination Summary**

| | |
|---|---|
| empirical formula | $C_{84}H_{74}Mo_{12}N_2O_{42}PS_{64}$ |
| color, habit | black, prisms |
| crystal size (mm) | 0.3 × 0.3 × 0.3 mm |
| crystal system | monoclinic |
| space group | *I*2 |
| unit-cell dimensions | $a = 14.086(6)$ Å<br>$b = 43.260(10)$ Å<br>$c = 14.062(6)$ Å<br>$\beta = 107.84(4)°$ |
| volume | 8157(5) Å$^3$ |
| *Z* | 2 |
| formula wt | 5017.5 |
| density (calc) | 2.043 Mg/m$^3$ |
| abs coeff | 1.787 mm$^{-1}$ |
| *F*(000) | 4942 |
| diffractometer used | Nicolet automated four-circle |
| radiation | MoKα ($\lambda = 0.71069$ Å) |
| temp (K) | 293 |
| monochromator | highly oriented graphite crystal |
| 2θ range | 3.0−55.0° |
| scan type | 2θ−θ |
| standard reflections | 2 measured every 50 reflections |
| index ranges | $0 \le h \le 18$, $0 \le k \le 49$,<br>$-18 \le l \le 17$ |
| reflections collected | 6270 |
| independent reflections | 5929 ($R_{int} = 5.9\%$) |
| observed reflections | 4788 ($F > 6.0\sigma(F)$) |
| system used | Siemens SHELXTL PLUS (PC version) |
| solution | Patterson and Fourier analysis |
| quantity minimized | $\sum w(F_o - F_c)^2$ |
| weighting scheme | $w^{-1} = \sigma^2(F) + 0.0015F^2$ |
| no. of parameters | 1040 |
| final *R* indexes (obs data) | $R = 6.46\%$, $wR = 8.30\%$ |
| goodness-of-fit | 1.57 |

(6) (a) Attanasio, D.; Bellitto, C.; Bonamico, M.; Fares, V.; Imperatori, P.; Patrizio, S. *M.R.S. Symp. Proc.* **1989**, *173*, 143. (b) Attanasio, D.; Bellitto, C.; Bonamico, M.; Fares, V.; Imperatori, P. *Gazz. Chim. Ital.* **1991**, *121*, 155. (c) Attanasio, D.; Bellitto, C.; Bonamico, M.; Fares, V.; Patrizio, S. *Synth. Met.* **1991**, *41–43*, 2289. (d) Attanasio, D.; Bellitto, C.; Bonamico, M.; Righini, G.; Staulo, G. *M.R.S. Symp. Proc.* **1992**, *247*, 545.

(7) Day, P.; Kurmoo, M.; Mallah, T.; Marsden, R.; Friend, R. H.; Pratt, F. L.; Hayes, W.; Chasseau, D.; Gaultier, J.; Bravic, G.; Ducasse, L. *J. Am. Chem. Soc.* **1992**, *114*, 10722 and reference therein.

(8) (a) Keggin, J. F. *Proc. R. Soc. London* **1934**, *A144*, 75. (b) For a recent review see: Pope, M. T.; Müller, A. *Angew. Chem., Int. Ed. Engl.* **1991**, *30*, 34.

(9) Robin, M. B.; Day, P. *Adv. Inorg. Chem. Radiochem.* **1967**, *10*, 247.

(10) (a) Bellitto, C.; Bonamico, M.; Staulo, G. *Mol. Cryst. Liq. Cryst.* **1993**, *232*, 155. (b) Kurmoo, M.; Day, P.; Bellitto, C. *Synth. Met.* **1995**, *70*, 963.

(11) Davidson, A.; Boubekeur, K.; Penicaud, A.; Auban, P.; Lenoir, C.; Batail, P.; Hervé, G. *J. Chem. Soc., Chem. Commun.* **1989**, 1373.

(12) Larsen, J.; Lenoir, C. *Synthesis* **1989**, *2*, 134.

(13) Sanchez, C.; Livage, J.; Launay, J. P.; Fournier; Jeannin, Y. *J. Am. Chem. Soc.* **1982**, *104*, 3194.

respectively. A detailed discussion of this disorder is reported as a supporting information. Difference syntheses showed additional electron density in the large holes present between the polyoxoanions. Several alternate cycles of Fourier difference syntheses and least-squares refinements finally allow the identification of the solvent as acetonitrile and water molecules and their occupancy factors. In the case of the acetonitrile molecule, it was necessary to use a rigid-body least squares refinement, using standard distances and angles. It was not possible to locate the hydrogen atoms. Anisotropic thermal parameters were refined for all the atoms except the carbon and the disordered atoms with occupancy factor of $^1/_3$, for which isotropic refinement was used. Cycles of least-squares gave a final $R$ and $R_w$ values of 6.46 and 8.30%, respectively. Difference Fourier map calculated after final refinement gives residual electron density of ±1 e Å$^{-3}$. Atomic coordinates and equivalent isotropic thermal parameters are given in Table 2. Bond lengths and angles and anisotropic temperature factors have been deposited as supporting information.

X-ray powder diffraction data were collected on a Seifert XRD-3000 with flat plate sample, curved graphite-single-crystal monochromator (Cu Kα = 1.542 Å), position sensitive detector operating in constant scan mode at 0.5° min$^{-1}$ over the range 3° < 2Θ < 80°. The diffractometer zero-point was determined from an external Si standard.

**X-ray Photoelectron Spectra.** A VG ESCA 3KII using Al Kα (1486.6 eV) was used. Samples were mounted on a gold holder, whose Au $4f_{7/2}$ line at 83.9 eV was used to check the instrumental scale. Analysis for peak position and width was performed by using a nonlinear least-squares program without background subtraction.[14]

**Electrical Conductivity.** Electrical conductivity measurements were performed on single crystals by the dc method as a function of temperature using an Oxford Instruments continuous flow cryostat. Temperature was measured by a calibrated Rh−Fe sensor. Contacts were made with platinum paint and arranged along three orthogonal axes of different crystals.

**Optical Measurements.** Infrared spectra at room temperature were recorded on a Perkin-Elmer 621 spectrophotometer on powdered samples both as Nujol mulls and KBr pellets. Optical reflectivity was measured on a Perkin-Elmer 1710 spectrometer equipped with an IR-plan microscope operating in the range 400−4300 cm$^{-1}$. The data were normalized to that of a gold mirror. A KRS5 polarizer was employed. A Cary 5 spectrophotometer was used to record diffuse reflectance spectra on diluted sample with MgO.

**Electron Paramagnetic Resonance.** X-band EPR spectra have been recorded in the temperature range 4−300 K by using a Varian E9 reflection spectrometer equipped with an Oxford Instrument cryostat and an ITC4 temperature controller. The single crystals were mounted on a Spectrosil quartz rod with silicone grease, and the powder samples were held in sealed 5 mm Spectrosil quartz tube containing helium exchange gas. Angular dependence of the EPR spectra was measured by use of a homemade goniometer. The field was calibrated with a DPPH standard.

(14) Mattogno, G.; Righini, G. *Surf. Interfac. Anal.* **1991**, *17*, 689.

**Static Magnetic Susceptibility.** Magnetic susceptibility measurements were performed by using a Quantum Design SQUID magnetometer in fields up to 5 T. The polycrystalline sample was placed inside a cellulose capsule in a polyethylene straw. All data are corrected for the core magnetization using Pascal's constants.

## Results and Discussion

**Electrochemical Reduction.** The α-Keggin anion $(NEt_4)_3[PMo_{12}O_{40}]$ shows two well-defined quasi-reversible waves at $E_{1/2}$ = +0.31 V [4−/3−] and at −0.11 V [5−/4−]. The separation of the anodic and cathodic $E_p$ is 0.07 V. The color of the solution changes from yellow to green at the first step and to blue at the second; each corresponds to a one-electron reduction. Another wave is observed at −0.85 V. Cyclic voltammograms for $TTF^0$ and BEDT-$TTF^0$ give $E_{1/2}$ = +0.46 and +0.59 V, respectively, for the first one-electron oxidation. The reversible $[PMo_{12}O_{40}]^{4-/3-}$ couple occurs at a slightly lower potential than that of $TTF^{0/+}$, suggesting energetically favorable chemical reaction between the $TTF^0$ molecule and the 3-charged anion, which is confirmed experimentally.[6c] $(NEt_4)_4[SiW_{12}O_{40}]$ shows two waves at −0.69 V ($E_p$ = 0.08 V) [5−/4−] and −1.19 V [6−/5−]. The first wave is reversible. The potentials are much higher than that of BEDT-TTF indicating that chemical oxidation of the latter on mixing with a solution of the cluster is unlikely.

**Crystal Growth.** In the electrochemical cell with $[PMo_{12}O_{40}]^{3-}$ as electrolyte there are three possible oxidation−reduction reactions taking place. At the cathode the anion is reduced to 4− and 5−. At the anode the BEDT-TTF is oxidized to the 1+ to form crystals with the 4− anion. The bulk of 4− salt crystallises on the cathode. In the case of $[SiW_{12}O_{40}]^{4-}$ there is no reduction of the anion since the working potential is small. It is important to note that crystals are formed with the reduced anion in the anodic part of the cell. Such an observation is made for the first time.

**Crystal Structure of $(BEDT\text{-}TTF)_8[PMo_{12}O_{40}]\cdot\{(CH_3CN\cdot H_2O)_2\}$.** The exact stoichiometry of the compound was determined by refinement of the crystal structure. The crystal structure consists of BEDT-TTF layers, which alternate along the $b$ axis with layers of the polyoxoanions having the α-Keggin structure. Water and acetonitrile molecules are located in the interstitial spaces within the anion layers. As mentioned in the Experimental Section, the crystal structure is disordered. Such disorder can be described as due to the superposition of three sublattices, i.e., A, B, and B′. In the A sublattice (see Figure 1a) the cations are located as in the silicotungstate derivative.[11] In the B sublattice (see Figure 1b) the cations are rotated by ~45° compared to those in the A sublattice, with an occupancy of $^2/_3$. An analysis of their atomic coordinates reveals a pseudoinversion center between them, which can be interpreted as due to the 2-fold disorder caused by the superposition of two centrosymmetrically related sublattices B and B′, each having occupancy factor $^1/_3$.

The BEDT-TTF layer structure is a pseudo-α-phase. Similar to $(BEDT\text{-}TTF)_8[SiW_{12}O_{40}]$[11] and $(BEDT\text{-}TTF)_8$-

**Table 2. Atomic Coordinates ($\times 10^4$) and Equivalent Isotropic Displacement Coefficients ($Å^2 \times 10^3$)[a]**

| | x | y | z | U(eq) | | x | y | z | U(eq) |
|---|---|---|---|---|---|---|---|---|---|
| P | 0 | 0 | 0 | 18(2) | C(28) | 3891(35) | 3489(11) | 3216(34) | 49(13) |
| Mo(1) | 1832(2) | −611(1) | 278(2) | 32(1) | C(29) | 3784(23) | 1947(7) | 3717(22) | 32(7) |
| Mo(2) | −259(2) | −605(1) | −1855(2) | 41(1) | C(2T) | 3783(19) | 2282(6) | 3745(18) | 19(5) |
| Mo(3) | 2142(1) | −21(1) | 2139(1) | 37(1) | C(31) | 323(28) | 1113(9) | 4643(27) | 29(9) |
| Mo(4) | 1579(1) | −33(1) | −1545(1) | 46(1) | C(33) | 24(26) | 1776(8) | 4530(25) | 21(8) |
| Mo(5) | 1857(2) | 553(1) | 309(2) | 46(1) | C(35) | 256(25) | 3244(8) | 4668(24) | 10(8) |
| Mo(6) | 306(2) | 548(1) | 1866(2) | 36(1) | C(37) | 496(28) | 3845(9) | 4838(28) | 23(9) |
| O(1a)[b] | 765(18) | 182(7) | 785(19) | 15(7) | C(39) | 0 | 2312(9) | 5000 | 17(8) |
| O(2a)[b] | 539(19) | −236(5) | −526(17) | 10(6) | C(3T) | 0 | 2629(16) | 5000 | 75(19) |
| O(1b)[c] | −746(68) | −210(21) | −658(65) | 49(23) | C(41) | 2750(23) | 1096(7) | 7155(23) | 14(7) |
| O(2b)[c] | −571(63) | 228(19) | 652(59) | 53(21) | C(42) | 1971(30) | 1122(10) | 7690(30) | 29(10) |
| O(3) | 2590(20) | −867(7) | 540(25) | 79(13) | C(43) | 2540(36) | 1757(12) | 7006(36) | 49(13) |
| O(4) | −387(22) | −897(7) | −2723(21) | 66(11) | C(44) | 2435(26) | 1781(8) | 7999(25) | 21(8) |
| O(5) | 3109(13) | −69(9) | 3114(12) | 87(11) | C(45) | 2767(30) | 3235(9) | 7099(29) | 28(10) |
| O(6) | 2306(13) | −36(10) | −2274(12) | 66(8) | C(46) | 2296(29) | 3231(9) | 7861(28) | 13(9) |
| O(7) | 2756(13) | 837(4) | 377(17) | 28(7) | C(47) | 2795(26) | 3858(9) | 7137(26) | 19(8) |
| O(8) | 444(25) | 801(6) | 2681(16) | 59(11) | C(48) | 1953(35) | 3860(11) | 7576(34) | 49(12) |
| O(9) | 730(12) | −744(6) | −707(12) | 64(9) | C(49) | 2565(18) | 2334(6) | 7519(18) | 17(6) |
| O(10) | 2417(18) | −335(5) | 1422(19) | 79(11) | C(4T) | 2612(25) | 2651(8) | 7521(25) | 48(9) |
| O(11) | 2273(14) | −377(4) | −687(13) | 38(7) | C(51) | 4810(33) | 1138(10) | 439(33) | 43(11) |
| O(12) | 1099(17) | −750(6) | 1223(17) | 49(9) | C(53) | 4978(27) | 1758(9) | 533(26) | 22(9) |
| O(13) | −1145(13) | −293(4) | −2280(12) | 37(7) | C(55) | 4716(29) | 3233(9) | 375(28) | 28(9) |
| O(14) | 677(16) | −378(4) | −2328(14) | 47(8) | C(57) | 4399(35) | 3821(11) | 116(35) | 35(12) |
| O(15) | 2513(13) | 276(4) | 1282(13) | 57(8) | C(59) | 5000 | 2311(8) | 0 | 19(7) |
| O(16) | 2118(16) | 222(5) | −456(16) | 49(8) | C(5T) | 5000 | 2618(16) | 0 | 73(20) |
| O(17) | 545(15) | 235(4) | −2037(12) | 39(7) | S(111) | 1021(17) | 1812(5) | 2420(16) | 38(5) |
| O(18) | 923(12) | 738(4) | −903(13) | 57(7) | S(112) | 1782(18) | 1803(5) | 279(18) | 38(5) |
| O(19) | 1479(14) | 302(3) | 2636(10) | 28(6) | S(113) | 1054(16) | 2465(5) | 2230(16) | 32(5) |
| O(20) | 1187(22) | 733(6) | 1053(18) | 65(11) | S(114) | 1391(14) | 2456(4) | 173(14) | 23(4) |
| S(11) | 134(9) | 1812(2) | 1632(8) | 26(4) | S(115) | 889(24) | 3180(7) | 2020(24) | 53(8) |
| S(12) | 2410(12) | 1822(4) | 1076(14) | 58(7) | S(116) | 1334(16) | 3208(5) | 133(16) | 32(5) |
| S(13) | 272(11) | 2500(3) | 1462(12) | 36(5) | S(117) | 848(17) | 3866(5) | 2336(16) | 32(5) |
| S(14) | 2066(11) | 2495(3) | 936(12) | 40(5) | S(118) | 1465(20) | 3885(6) | 92(19) | 40(7) |
| S(15) | 192(10) | 3246(2) | 1481(9) | 30(4) | S(121) | 3377(17) | 1047(5) | 4843(16) | 29(5) |
| S(16) | 2109(14) | 3244(3) | 909(12) | 54(6) | S(122) | 4034(23) | 1053(7) | 2708(22) | 51(8) |
| S(17) | 72(11) | 3914(3) | 1592(12) | 43(5) | S(123) | 3507(18) | 1721(5) | 4699(17) | 28(5) |
| S(18) | 2284(14) | 3920(3) | 834(13) | 61(7) | S(124) | 4147(16) | 1726(5) | 2930(16) | 22(4) |
| S(21) | 2673(9) | 1088(3) | 4088(12) | 40(5) | S(125) | 3390(25) | 2465(7) | 4611(24) | 59(9) |
| S(22) | 4807(11) | 1067(4) | 3475(14) | 54(6) | S(126) | 4185(21) | 2477(6) | 3045(19) | 43(6) |
| S(23) | 2900(9) | 1769(3) | 4102(11) | 31(4) | S(127) | 3400(16) | 2148(5) | 4944(16) | 31(5) |
| S(24) | 4740(10) | 1766(3) | 3605(12) | 41(5) | S(128) | 3724(17) | 3158(5) | 2507(17) | 39(6) |
| S(25) | 2785(11) | 2506(3) | 3970(12) | 39(5) | S(131) | 1195(17) | 1422(6) | 4837(18) | 41(6) |
| S(26) | 4759(12) | 2513(3) | 3544(13) | 38(5) | S(133) | 894(18) | 2080(5) | 4629(19) | 36(5) |
| S(27) | 2582(12) | 3175(3) | 3861(13) | 50(6) | S(135) | 995(23) | 2847(7) | 4883(22) | 59(8) |
| S(28) | 4802(14) | 3181(5) | 3333(15) | 84(9) | S(137) | 1057(15) | 3514(5) | 4556(15) | 18(4) |
| S(31) | 424(12) | 1459(3) | 3936(11) | 35(5) | S(141) | 3553(21) | 1406(7) | 7087(21) | 46(7) |
| S(33) | 218(13) | 2136(3) | 4077(11) | 40(5) | S(142) | 1402(24) | 1409(8) | 7969(23) | 60(8) |
| S(35) | 273(13) | 2882(3) | 4030(10) | 38(5) | S(143) | 3334(19) | 2075(5) | 7082(19) | 33(5) |
| S(37) | 339(15) | 3561(4) | 3907(13) | 51(6) | S(144) | 1580(19) | 2093(5) | 7820(19) | 35(6) |
| S(41) | 2787(12) | 1449(4) | 6412(11) | 45(5) | S(145) | 3531(23) | 2840(7) | 7402(22) | 54(8) |
| S(42) | 2194(10) | 1437(3) | 8683(11) | 45(5) | S(146) | 1516(15) | 2838(5) | 7636(15) | 32(5) |
| S(43) | 2739(14) | 2133(3) | 6539(12) | 47(6) | S(147) | 3680(14) | 3509(5) | 7258(14) | 22(4) |
| S(44) | 2264(12) | 2128(3) | 8442(12) | 41(6) | S(148) | 1400(17) | 3498(5) | 7759(16) | 31(5) |
| S(45) | 2722(14) | 2875(3) | 6510(10) | 49(6) | S(151) | 3847(18) | 1438(6) | 226(17) | 39(6) |
| S(46) | 2232(12) | 2883(3) | 8401(10) | 36(5) | S(153) | 4129(16) | 2108(5) | 356(17) | 22(4) |
| S(47) | 2788(15) | 3541(4) | 6393(10) | 61(7) | S(155) | 4083(20) | 2832(6) | 118(20) | 48(7) |
| S(48) | 2129(15) | 3549(4) | 8585(11) | 51(6) | S(157) | 3937(16) | 3522(5) | 427(16) | 25(4) |
| S(51) | 4699(14) | 1455(3) | 1115(11) | 43(5) | C(111) | 893(62) | 1510(20) | 1612(61) | 20(19) |
| S(53) | 4762(13) | 2127(3) | 901(11) | 41(5) | C(112) | 1736(67) | 1490(21) | 1074(63) | 27(21) |
| S(55) | 4701(13) | 2868(3) | 934(11) | 42(5) | C(113) | 1129(83) | 2058(26) | 1634(81) | 59(29) |
| S(57) | 4732(12) | 3550(3) | 1122(10) | 38(5) | C(114) | 1518(63) | 2087(21) | 815(63) | 44(21) |
| C(11) | 791(24) | 1476(8) | 1499(23) | 24(7) | C(115) | 1103(86) | 3560(27) | 1529(85) | 21(30) |
| C(12) | 1572(30) | 1464(10) | 811(29) | 34(10) | C(116) | 1269(97) | 3543(33) | 1027(95) | 80(37) |
| C(13) | 693(26) | 2111(8) | 1340(26) | 22(8) | C(117) | 997(74) | 4225(23) | 1331(72) | 24(25) |
| C(14) | 1693(19) | 2114(6) | 1156(20) | 16(5) | C(118) | 1455(72) | 4217(23) | 1033(68) | 54(24) |
| C(15) | 796(35) | 3599(11) | 1253(32) | 34(11) | C(121) | 3120(64) | 778(20) | 3893(60) | 20(20) |
| C(16) | 1480(22) | 3581(7) | 967(21) | 12(6) | C(122) | 3397(76) | 778(23) | 2950(73) | 62(25) |
| C(17) | 1174(33) | 4187(11) | 1847(32) | 41(10) | C(123) | 3744(61) | 1349(21) | 4372(61) | 20(19) |
| C(18) | 1535(29) | 4217(9) | 1034(28) | 38(9) | C(124) | 4002(67) | 1381(22) | 3333(64) | 36(21) |
| C(19) | 1148(25) | 2708(8) | 1130(23) | 40(8) | C(125) | 3675(84) | 2774(26) | 4236(83) | 20(31) |
| C(1T) | 1142(18) | 2997(6) | 1094(17) | 19(5) | C(126) | 3707(71) | 2825(23) | 3278(69) | 38(23) |
| C(21) | 3032(33) | 806(10) | 3401(32) | 54(11) | C(127) | 3203(101) | 3474(32) | 3840(96) | 93(41) |
| C(22) | 4016(57) | 768(18) | 3277(54) | 73(24) | C(128) | 4285(96) | 3538(31) | 3849(88) | 92(38) |
| C(23) | 3288(26) | 1390(9) | 3894(25) | 25(9) | C(131) | 183(51) | 1138(16) | 4485(51) | 23(15) |
| C(24) | 4237(36) | 1389(12) | 3629(34) | 36(12) | C(133) | 395(71) | 1732(22) | 4830(70) | 75(23) |
| C(25) | 3258(62) | 2837(19) | 3613(57) | 92(27) | C(135) | 399(70) | 3205(22) | 4718(69) | 31(23) |
| C(26) | 4008(24) | 2828(7) | 3434(22) | 15(7) | C(137) | 211(77) | 3801(24) | 4562(73) | 59(25) |
| C(27) | 3584(27) | 3446(9) | 4133(26) | 27(8) | C(141) | 2751(80) | 1146(24) | 7106(76) | 56(29) |

**Table 2 (Continued)**

| | *x* | *y* | *z* | *U*(eq) | | *x* | *y* | *z* | *U*(eq) |
|---|---|---|---|---|---|---|---|---|---|
| C(142) | 2348(90) | 1112(28) | 8116(88) | 60(34) | N(3)[c] | −312(36) | −326(15) | 4987(59) | 74(22) |
| C(143) | 2826(80) | 1727(25) | 7462(76) | 49(28) | C(6)[c] | −1148 | −380 | 4843 | 41(19) |
| C(144) | 2029(71) | 1714(22) | 7618(69) | 32(24) | C(5)[c] | −2203 | −448 | 4662 | 32(15) |
| C(145) | 2903(71) | 3199(22) | 7404(70) | 37(23) | N(4)[c] | 4553(38) | 331(12) | −198(32) | 38(14) |
| C(146) | 2082(72) | 3199(22) | 7604(70) | 21(23) | C(8)[c] | 4461 | 379 | −1030 | 64(27) |
| C(147) | 2919(84) | 3862(27) | 7303(81) | 103(32) | C(7)[c] | 4346 | 440 | −2079 | 11(11) |
| C(148) | 2286(76) | 3837(24) | 7945(75) | 66(27) | C(9)[c] | 4495(41) | 405(17) | 6924(46) | 39(18) |
| C(151) | 4637(83) | 1037(26) | 458(80) | 57(28) | C(10)[c] | 3514 | 415 | 6178 | 58(23) |
| C(153) | 4613(80) | 1742(26) | −18(80) | 32(29) | N(5)[c] | 2735 | 423 | 5586 | 54(18) |
| C(155) | 4503(71) | 3221(22) | 56(75) | 50(25) | N(6)[c] | −464(30) | 343(11) | 4468(34) | 29(12) |
| C(157) | 4718(67) | 3855(21) | 283(63) | 42(23) | C(T1)[c] | −2347 | 445 | 4259 | 17(13) |
| C(1)[c] | 4705(79) | −429(24) | −2150(59) | 63(29) | C(T2)[c] | −1297 | 388 | 4376 | 36(16) |
| C(2)[c] | 4694 | −362 | −1137 | 96(37) | O(w)[b] | 5692(16) | 63(6) | 4277(15) | 54(12) |
| N(1)[c] | 4686 | −310 | −333 | 71(42) | O(w1)[c] | 5031(37) | −377(12) | 1660(35) | 37(12) |
| N(2)[c] | 4331(46) | −482(16) | 7564(36) | 48(20) | O(w3)[c] | 1689(26) | −379(9) | 5111(28) | 13(8) |
| C(4)[c] | 3858 | −481 | 6731 | 56(22) | O(w4)[c] | 5429(28) | 386(9) | 1647(30) | 10(8) |
| C(3)[c] | 3262 | −479 | 5681 | 19(12) | O(w6)[c] | 1779(24) | 409(8) | 5454(23) | 10(6) |

[a] Note that for the BEDT-TTF molecules whose orientation has occupation factor (o.f.) = $^2/_3$, the first figure in the numbering of the S and C atoms indicates the molecule in Figure 1b. The central C atoms of sublattice A [with last figure = 9 or *T* (=10)] are indistinguishable from those of sublattice B: therefore the latter were computed with an o.f. = 1, apart from molecules (3) and (5) in which they are in special positions and consequently their o.f. were = 0.5. For the cations with o.f. = $^1/_3$, the atomic numbering is made up of three figures: the first two figures indicate the molecular number reported in Figure 1a. [b] Other atoms with o.f. = $^2/_3$. [c] Other atoms with o.f. = $^1/_3$.

$[CoW_{12}O_{40}]\cdot 5.5H_2O$[15] the BEDT-TTF molecules form two different types of chain in the organic layers; chain I contains three crystallographically independent molecules (3, 4, 5) packed in an eclipsed mode, the shortest S−S distances being 4.01(2) Å. In chain II, two independent molecules (1, 2) are present: the binary axes connect two pairs of molecules which are disposed in a zigzag mode along the [101] direction. The shortest intradimer and interdimer S−S distances are 3.77(2), 3.89(2), and 3.97(2) Å, respectively. The shortest S−S interchain contacts are shorter than those within the chain, and they range between 3.41(2) and 3.58(2) Å as observed in similar compounds. These distances are referred to the B sublattice and very similar values are observed in the A sublattice. A supplementary disorder is also found in some ethylene groups, as commonly observed in BEDT-TTF salts.

The anions are located on the 2-fold axis, as observed in the α-Keggin structure, but Mo−Mo distances are unusual because of the disorder. In the α-Keggin structures the $T_d$ symmetry determines two types of metal−metal distances and in the molybdenum salts they are 3.40 and 3.70 Å, respectively; in a "pseudo-Keggin" molecule with $m3m$ ($O_h$) symmetry,[16] all the metal−metal distances are equivalent and in the molybdenum structure the distance is 3.55 Å. In the present case $T_d$ symmetry is preserved, but the difference between the two Mo−Mo observed distances, i.e., 3.50(1) and 3.60(1) Å, is smaller than in the α-Keggin structure. Such values can be obtained considering the superposition of the acentric α-Keggin structure belonging to the A sublattice ($^1/_3$ occupancy factor), with those centrosymmetrically related to the B and B′ sublattices. The weighted averages between the short (3.4 Å) and the long (3.7 Å) distances of the α-Keggin molecule with that (3.55 Å) of the centrosymmetric "pseudo-Keggin" structure give values of 3.50 and 3.60 Å, in agreement with those found in this structure. Such disordered superposition leads to a spread in the values of Mo−O distances: e.g., for terminal oxygens they are in the range 1.55(2)−1.74(2) Å, and for the doubly bridged they are 1.79(3)−2.09(3) Å. The Mo−O distances with oxygens of the $PO_4$ group are 2.42(2)−2.50(2) Å.

Water and acetonitrile molecules are located in large holes made up by the α-Keggin anions. Figure 2 shows the superposition of disordered solvent molecules: for clarity, atomic positions generated by the binary axis at 0, 0, $^1/_2$ and $^1/_2$, 0, 0 are omitted. Acetonitrile molecules drawn with solid lines form hydrogen bonds with the water molecules. Those drawn with dotted lines in Figure 2 are not involved in hydrogen bonding and by steric considerations must be referred to the A sublattice. Consequently the rest of the solvent molecules belong to the B and B′ sublattices. As observed in other solvated polyoxoanions derivatives of organic cations,[17,18] in the present case there is no specific interactions between the solvent molecules and the anions.

**X-ray Photoelectron Spectra.** In all the salts studied the molybdenum atoms are equivalent and the value of the binding energy Mo $3d_{3/2,5/2}$ are 232.8(0.2) and 236(0.4) eV. W $4f_{7/2}$ is observed at 35.5 eV. The existence of one $Mo^V$ or $W^V$ in the cluster (see EPR section) cannot be ruled out if it corresponds to class IIIA of the Robin and Day scheme.[9] In this case the shift in energy would be very small as the extra electron would be delocalized over all the 12 molybdenum atoms (cf. magnetic data).

The observed spectrum for BEDT-TTF derivative shows the peak corresponding to S $2p_{3/2}$ (164.0(2) eV) and the shoulder attributed to $S2p_{1/2}$. The fwhm is <2 eV, suggesting the presence of one type of sulfur and an effective charge of +0.5.[19] The quantitative analysis of the intensity of S 2p and of metal peaks gave the atomic ratio S/metal of $^{64}/_{12}$ as expected from crystallography.

(15) Gomez-Garcia, C. J.; Ouahab, L.; Gimenez-Saiz, C.; Triki, S.; Coronado, E.; Delhaes, P. *Angew. Chem., Int. Engl. Ed.* **1994**, *33*, 223.
(16) Evans, H. T.; Pope, M. T. *Inorg. Chem.* **1984**, *23*, 501.
(17) Bonamico, M.; Attanasio, D.; Fares, V.; Imperatori, P.; Suber, L. *J. Chem. Soc. Dalton* **1990**, 3221.
(18) Williamson, M. W.; Bouchard, D. A.; Hill, L. G. *Inorg. Chem.* **1987**, *26*, 1436.
(19) Bellitto, C.; Staulo, G.; Bozio, R.; Pecile, C. *Mol. Cryst. Liq. Cryst.* **1993**, *234*, 205.
(20) Pope, M. T. In *Mixed-valence Compounds*; Brown, D. B., Ed.; NATO ASI; 1980, Vol. C58, p 365.

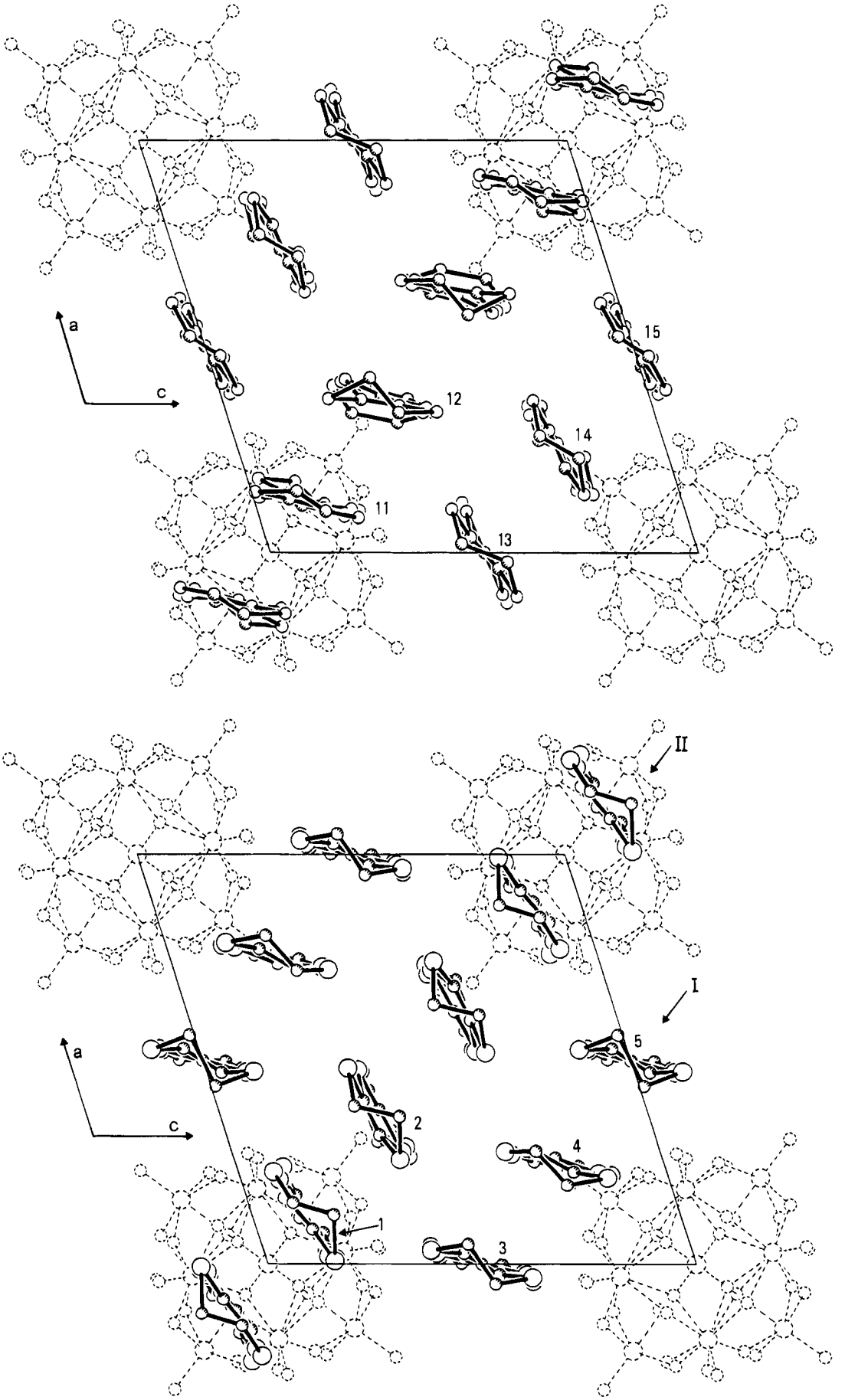


**Figure 1.** (a, top) A sublattice of $(BEDT\text{-}TTF)_8[PMo_{12}O_{40}]\cdot\{(CH_3CN\cdot H_2O)_2\}$ projected along [010] showing both the inorganic and organic layer. (b, bottom) B sublattice projected along [010] showing the different orientation of the BEDT-TTF molecules, with respect to A. The solvent molecules are omitted for clarity.

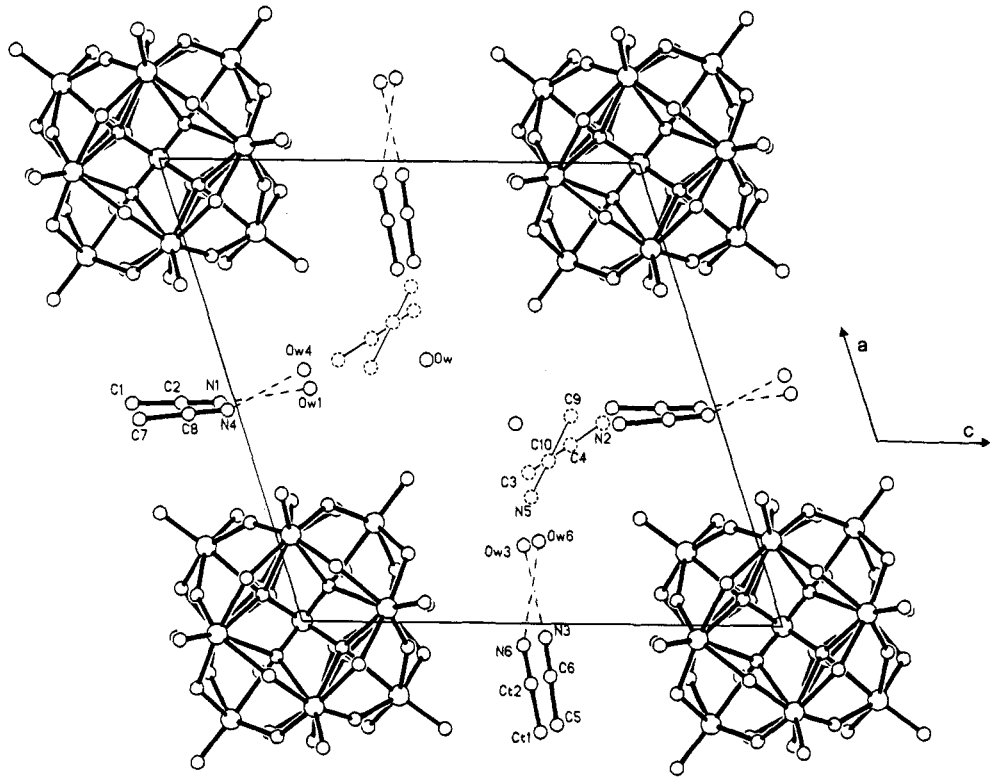


**Figure 2.** Inorganic layer projected along [010] with the location of the solvent molecules (partial view).

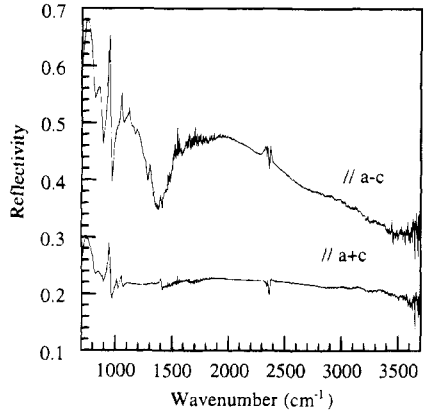


**Figure 3.** Polarized single-crystal reflectivity spectra of $(BEDT\text{-}TTF)_8[PMo_{12}O_{40}]\cdot\{(CH_3CN\cdot H_2O)_2\}$ in the mid-infrared region.

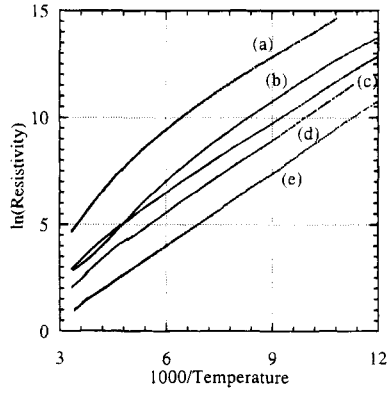


**Figure 4.** Temperature dependence of the electrical resistance (a) along $b^*$, (b) along $a + c$, and (c) along the $a-c$ directions of $(BEDT\text{-}TTF)_8[PMo_{12}O_{40}]\cdot\{(CH_3CN\cdot H_2O)_2\}$ and (d) along $a + c$ and (e) along $a-c$ of $(BEDT\text{-}TTF)_8[SiW_{12}O_{40}]$ single crystals.

**Optical Spectra.** In the $(BEDT\text{-}TTF)_8[XM_{12}O_{40}]$ compounds[6d] a strong polarized band (Figure 3) at ~2000 $cm^{-1}$ (~0.25 eV) is observed, which is characteristic of mixed-valence intermolecular excitation from the organic moiety.[21] The polarization-dependent reflectivity confirms the anisotropy of the conductivity and charge-transfer processes.[22] The vibrational spectrum of the anions is as expected. The dominant vibration from BEDT-TTF is about 1300 $cm^{-1}$, involving the C=C central bond.[22] This mode couples strongly to the charge oscillating between molecules of each dimer as exemplified by its Fano type structure as observed for $\beta''$-$(BEDT\text{-}TTF)_2AuBr_2$.[23] The energy of the bands and intensity corresponding to the anions are as expected for the 4-charge.[24]

**Electrical Conductivity.** *$(BEDT\text{-}TTF)_8[PMo_{12}O_{40}]\cdot\{(CH_3CN\cdot H_2O)_2\}$.* Measurements of conductivity were made on several crystals; the data were very reproducible. The contacts were aligned along three orthogonal directions, the long axis of the plate crystal ($a-c$), the short axis ($a + c$) and on the two flat faces ($b^*$) of the crystals. The anisotropy in the conductivity at ambient temperature for $(BEDT\text{-}TTF)_8[PMo_{12}O_{40}]\cdot\{(CH_3CN\cdot H_2O)_2\}$ is $\sigma$ = 0.1, 0.05, 0.009 S $cm^{-1}$, respectively. Figure 4 shows the experimental values of ln $\varrho$ vs inverse temperature. The behavior along the long axis and between the two faces is similar, whereas that along the short axis is different. The former two cases show

(21) Torrance, J. B.; Scott, B. A.; Weber, B.; Kaufmann, F. B.; Seiden, P. E. *Phys. Rev.* **1979**, *B19*, 730.
(22) Kornelsen, K.; Eldridge, J. E.; Wang, H. H.; Charlier, H. A.; Williams, J. M. *Solid State Commun.* **1992**, *81*, 343.
(23) Pratt, F. L.; Hayes, W.; Kurmoo, M.; Day, P. *Synth. Met.* **1988**, *27*, A439.
(24) (a) Rocchiccioli-Deltcheff, C.; Fournier, M.; Franck, R. *Inorg. Chem.* **1983**, *22*, 207. (b) Fournier, M.; Rocchiccioli-Delchieff, C.; Kazansky, L. P. *Chem. Phys. Lett.* **1994**, *223*, 297.

a temperature-dependent activation energy, while the latter has not. Similar temperature dependence resistivity has been observed in $(BEDT\text{-}TTF)_3CuBr_4$.[25] At low temperature the activation energy ($E_A = 0.088$ eV) is almost the same for all three directions. At ~175 K there is a gradual change in the slope, suggesting a possible phase transition whose width is very broad. The activation energy ($E_A = 0.177$ eV) above 200 K is twice that at low temperature. The temperature at the largest change in the slope corresponds to that where a second EPR signal begins to appear (see below).

*$(BEDT\text{-}TTF)_8[SiW_{12}O_{40}]$.* Measurements on several crystals give a room-temperature conductivity of 0.4 S $cm^{-1}$, a factor of 5 smaller than that found by Davidson et al.[11] The activation energy (0.098 eV) at high temperature is slightly lower than at low temperature, similar to that of $(BEDT\text{-}TTF)_8[PMo_{12}O_{40}]\{(CH_3CN\cdot H_2O)_2\}$ at low temperature. Although there appears to be a transition similar to that found in $(BEDT\text{-}TTF)_8[PMo_{12}O_{40}]\{(CH_3CN\cdot H_2O)_2\}$, the change in activation energy is not large. However, we find an activation energy that is one-third that found by Davidson et al.[11]

**Magnetic Properties.** The magnetic properties of the BEDT-TTF polyoxoanions have been studied by two methods, EPR and bulk susceptibility, the results of which are described and discussed separately. The EPR data clearly differentiate between the different phases.[10] Those for the $(BEDT\text{-}TTF)_8[PMo_{12}O_{40}]\cdot\{(CH_3CN\cdot H_2O)_2\}$ salt were quite unusual, and to understand them it is necessary to examine the EPR spectra of the paramagnetic mixed-valence $(NBu_4)_4[PMo_{12}O_{40}]$ on the one hand and of $(BEDT\text{-}TTF)_8[SiW_{12}O_{40}]$, where the anion is diamagnetic, on the other.

**Electron Paramagnetic Resonance.** At room temperature a polycrystalline sample of $(NBu_4)_4[PMo_{12}O_{40}]$ shows a broad resonance ($H_{pp} = 850 \pm 25$ G) centered at $g = 1.95$. At 100 K it is sharper ($g = 1.9444$) but still shows no hyperfine structure. It sharpens further to 62(2) G as the temperature is lowered to 13 K and weak satellites peaks appear. The $g$ values and line widths are close to those found previously for this compound.[13,26] However, the resonance in the solid state is not sufficiently resolved to allow assignment of the parallel and perpendicular components and the hyperfine constants. $(Et_4N)_4[SiW_{12}O_{40}]$ is EPR silent and thus diamagnetic as expected for an all $W^{VI}$ cluster.

The EPR spectra of a single crystal of $(BEDT\text{-}TTF)_8[SiW_{12}O_{40}]$ contain a single Lorentzian line, which increases in intensity as the temperature is lowered. The $g$ value is 2.006 ($H \| (ac)$plane) and 2.013 ($H \| b^*$) and the corresponding line widths are 28 and 45, respectively, at 300 K. These values are similar to those previously published.[11] The $[SiW_{12}O_{40}]^{4-}$ anion is diamagnetic, and therefore the signal is due only to the presence of spins localized on BEDT-TTF molecules. These $g$ values are constant in the temperature range studied and are in the range found for many BEDT-TTF salts with 0.5$e$+ charge.[27] The line width decreases

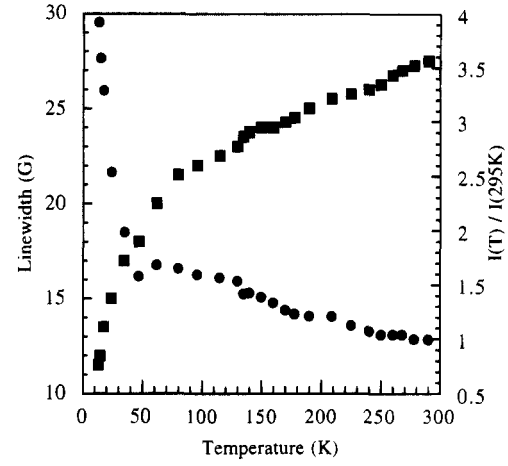


**Figure 5.** Temperature dependence of the EPR line width (squares) and spin susceptibility (circles) of $(BEDT\text{-}TTF)_8[SiW_{12}O_{40}]$.

linearly at a rate of 0.025 G/K to ca. 100 K (Figure 5). Below 100 K there is a more rapid drop to 11 G at 13 K. No hyperfine structure due to the $^{183}W$ ($I = 1/2$, 14.3% abundance) was observed. At low temperature the intensity approximately fits a Curie–Weiss law. At temperatures above 50 K, there is an indication of short-range order typical of low-dimensional antiferromagnets. If the relaxation rates and $g$ values are comparable, as in $(BEDT\text{-}TTF)_3CuBr_4$,[25] only one resonance will be observed, whose $g$ value will be given by[28]

$$g(\text{obs}) = [g(\text{BEDT-TTF})\chi(\text{BEDT-TTF}) + g(\text{anion})\chi(\text{anion})]/\chi(\text{total})$$

Otherwise separate resonances will be observed as in the case of $(BEDT\text{-}TTF)_3CuCl_4\cdot H_2O$.[7] The average $g$ value of $[SiW_{12}O_{40}]^{5-}$ is 1.821,[26] and the upper and lower limits for BEDT-TTF are 2.013 and 2.001. Using these values in the above equation for 1 anion spin per formula unit (see following section) and 7 spins from the conducting layers (if one assumes that each unit cell contains one $SiW_{12}O_{40}^{4-}$ and one $SiW_{12}O_{40}^{5-}$), we estimate the expected $g$ value in the range 1.976–1.986, still lower than the observed value. This suggests that the signal is purely organic and that the anion is diamagnetic.

EPR measurements on both a powdered sample and a single-crystal of $(BEDT\text{-}TTF)_8[PMo_{12}O_{40}]\{(CH_3CN\cdot H_2O)_2\}$ show a Lorentzian line which increases in intensity as the temperature is lowered. The $g$ values at room temperature are 2.002 ($H \| (a-c)$), 2.006 ($H \| (a+c)$) and 2.013 ($H \| b^*$). The line-width anisotropy is 31, 35, and 50 G, respectively. The $g$ values are typical of the BEDT-TTF radical and are close to the free electron value.[27] Making the same estimate as before with $g$(anion) as 1.944, we would expect a $g$ value in the range 1.988–1.996. In solution the EPR line of $PMo_{12}O_{40}^{4-}$ is isotropic, while in the BEDT-TTF salt the $g$ value is slightly anisotropic, suggesting a lowering of symmetry of the Mo coordination sphere. The spectra were also recorded at fixed orientations as a function of temperature. For all the crystal orientations studied, the single peak at room temperature splits into two peaks at about

(25) Marsden, I. R.; Allan, M. L.; Friend, R. H.; Kurmoo, M.; Kanazawa, D.; Day, P.; Bravic, G.; Chasseau, D.; Ducasse, L.; Hayes, W. *Phys. Rev.* **1994**, *B50*, 2118.

(26) (a) Fricke, R.; Öhlmann, G. *J. Chem. Soc., Faraday Trans. 1* **1986**, *82*, 263; *Ibid.* **1986**, *82*, 273. (b) Otake, M.; Komiyama, Y.; Otaki, T. *J. Phys. Chem.* **1973**, *24*, 2896. (c) Launay, J. P.; Fournier, M.; Sanchez, C.; Livage, J.; Pope, M. T. *Inorg. Nucl. Chem. Lett.* **1980**, *16*, 257. (d) Prados, R. A.; Pope, M. T. *Inorg. Chem.* **1979**, *15*, 2547.

(27) Sugano, T.; Saito; Kinoshita, M. *Phys. Rev.* **1986**, *34*, 117.

(28) Barnes, S. E. *Adv. Phys.* **1980**, *30*, 801.

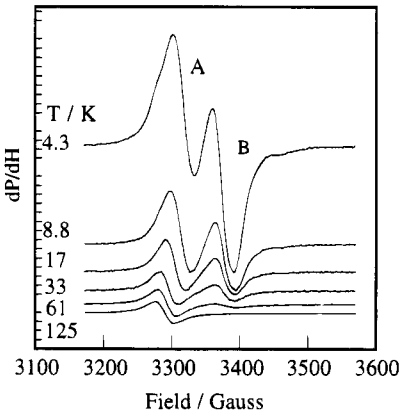


**Figure 6.** EPR spectra of a single crystal of $(BEDT\text{-}TTF)_8[PMo_{12}O_{40}]\{(CH_3CN{\cdot}H_2O)_2\}$ in the range 4−125 K.

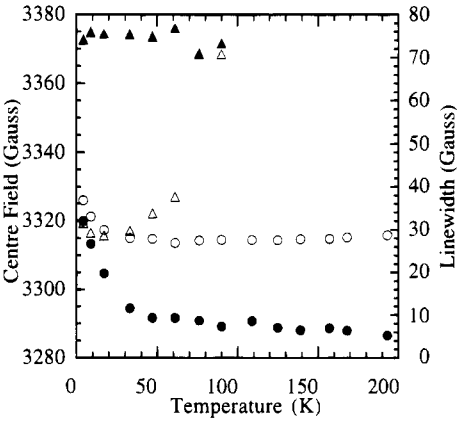


**Figure 7.** Temperature dependence of the (a) EPR line width (open circles and triangles) (b) resonance center field (filled circles and triangles) of the two signals of $(BEDT\text{-}TTF)_8[PMo_{12}O_{40}]\{(CH_3CN{\cdot}H_2O)_2\}$; circles are for peak A and triangles for peak B.

125 K; see Figure 6. The line width remains weakly anisotropic as do the $g$ values. On lowering the temperature, the intensity increases: in particular the peak at lower $g$ value grows in intensity at the expense of the first one. Close examination of the spectra at the lowest temperature (4.3 K) reveals fine structure on both peaks. These weak features are more pronounced in the second derivative spectrum and can be assigned to hyperfine coupling for $^{95}Mo$ ($I = {}^5/_2$; 15.9% natural abundance) and $^{97}Mo$ ($I = {}^5/_2$; 9.6%) isotopes. We do not observe any separate signal due to the BEDT-TTF radicals. Although, the $g$ value is close to that observed for BEDT-TTF salts, we associate the observed signal with both the BEDT-TTF and Mo(V) due to coupling between the two spin sublattices.

**Static Magnetic Susceptibility Measurements.** *$[PMo_{12}O_{40}]^{4-}$.* The magnetic susceptibility and isothermal magnetization of the tetraethylammonium (TEA) and tetrabutylammonium (TBA) salts have been measured. The molar susceptibility can be described by the relation

$$\chi_{anion} = \chi_{tip} + C_A/(T - \theta)$$

where $\chi_{tip}$ is the temperature-independent term and $C_A/(T - \theta)$ is Curie−Weiss law. The magnetization at 6 K and the fit to the susceptibilities indicate a larger value of $\theta$ for the TEA salt and different values of $\chi_{tip}$. For the TBA salt $C_A = 0.3402$ emu K/mol and $\chi_{tip} = 7 \times$

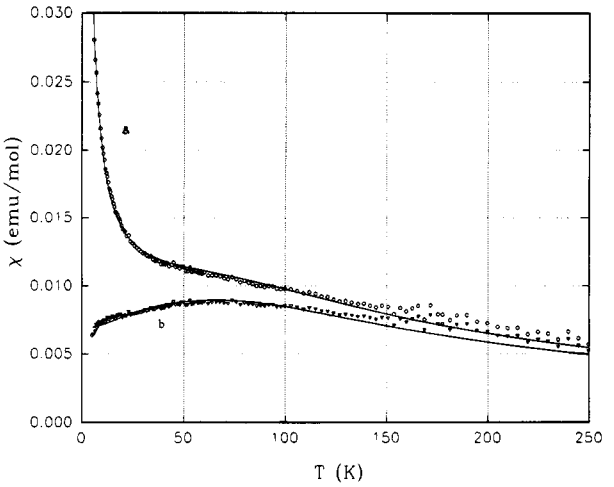


**Figure 8.** Temperature dependence of the (a) measured molar magnetic susceptibility and (b) after subtracting the Curie tail for $(BEDT\text{-}TTF)_8[SiW_{12}O_{40}]$; the solid line is the fit to the data.

$10^{-4}$ emu/mol have been found, consistent with low-lying mixed-valent transitions. The effective magnetic moment (1.65 $\mu_B$) is close to the theoretical value for $S = {}^1/_2$ and $g = 1.9444$.

*$(BEDT\text{-}TTF)_8[SiW_{12}O_{40}]$.* The temperature dependence of the magnetic susceptibility is shown in Figure 8. At 300 K the molar susceptibility is $5.7 \times 10^{-3}$ emu/mol, which is slightly higher than the susceptibility predicted by the Curie formula

$$\chi = A\{N(g^2\mu_B{}^2/3k_BT)S(S + 1)\}$$

where $A = 4$ is the number of unpaired electrons per formula unit and $S = {}^1/_2$. The effective magnetic moment at room temperature is 3.46 $\mu_B$, and it smoothly decreases with decreasing temperature. Below 100 K, it decreases rapidly, indicating antiferromagnetic coupling between the nearest-neighboring BEDT-TTF dimers. On the basis of the crystal structure, the experimental data were fitted to a model for a 1D Heisenberg antiferromagnet.[29-31] The best fit is obtained by assuming the presence of two different types of organic chains in the unit cell: one uniform and the other distorted. The molar magnetic susceptibility was then assumed to be the sum of three contributions:

$$\chi_{organic} = 2\chi_{uniform} + 2\chi_{distorted} + C_A/T$$

the first term being that of a uniform chain, the second for the zigzag dimers and the third resulting from paramagnetic impurities or odd segments present in the chains. The $g$ value for the organic was fixed to 2.0023. All the spins ($S = {}^1/_2$) were assumed to be localized and the number of the spin sites equal to the number of the BEDT-TTF dimers. The best fit was found assuming two types of chains: uniform ($\alpha = 1$)[30,31] and distorted ($\alpha = 0$) corresponds to the Bleaney−Bowers model for isolated dimer) with $J/k_B = -27$ K and $\Delta/k_B = -96.5$ K, respectively, and $C_A = 0.132$ emu K/mol. Another set

(29) (a) Obertelli, S. D.; Friend, R. H.; Talham, D.; Kurmoo, M.; Day, P. *J. Phys. Condens. Matter* **1989**, *1*, 5671. (b) Kurmoo, M.; Green, M. A.; Day, P.; Bellitto, C.; Staulo, G.; Pratt, F. L.; Hayes, W. *Synth. Met.* **1993**, *55–57*, 2380.
(30) Bonner, J. C.; Fisher, M. E. *Phys. Rev.* **1964**, *A135*, 640.
(31) Hall, J. W.; Marsh, W. E.; Weller, R. R.; Hatfield, W. E. *Inorg. Chem.* **1981**, *20*, 1033.

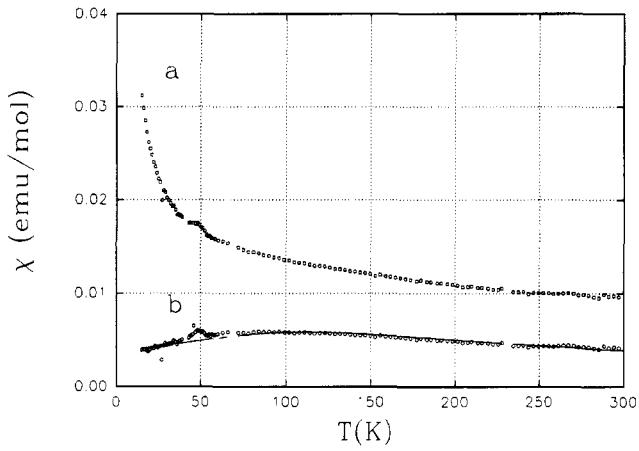


**Figure 9.** Temperature dependence of the (a) measured molar magnetic susceptibility and (b) after subtracting the cluster and the temperature-independent paramagnetic contribution for $(BEDT\text{-}TTF)_8[PMo_{12}O_{40}]\{(CH_3CN{\cdot}H_2O)_2\}$; the solid line is the fit to the data.

of data were also analyzed on the basis of the same model and similar values for $J/k_B$ and $\Delta/k_B$ were found but with a slightly different $C$ value (0.172) emu K/mol. The Curie-like tail at low temperature is always present, and it approximates to one-half spin per formula unit. Such a Curie tail is considered high but could be accounted if one assumes that one of the clusters in the unit cell is diamagnetic with charge 4− and the other is paramagnetic with a charge of 5−. This would then reduce the number of spins in the BEDT-TTF chains by one. However, the lack of fine structure from $^{183}W$ ($I = 1/2$) isotope and the $g$ value of the resonance disagree with this hypothesis. An alternative hypothesis is that the Curie tail originates from defects in the BEDT-TTF chains.

*$(BEDT\text{-}TTF)_8[PMo_{12}O_{40}]\{(CH_3CN{\cdot}H_2O)_2\}$.* The temperature variation of the magnetic susceptibility is shown in Figure 9. By plotting $1/\chi$ vs $T$ in the 2−20 K region a linear relationship is found with a $C$ value of 0.39 emu K/mol, indicating paramagnetism corresponding to one unpaired electron per formula unit. This result agrees with the EPR in indicating that the inorganic cluster contains one unpaired electron. If this contribution is subtracted from the total magnetic susceptibility, a curve showing a broad maximum at about 80 K is obtained (Figure 9). The value of the susceptibility $\chi$ at room temperature is slightly higher than that expected for four independent spins with $S = 1/2$ per formula unit ($5 \times 10^{-3}$ emu/mol). This indicates that temperature-independent paramagnetism, $\chi_{tip}$, is present, similar to that found in the one-electron-reduced anion salt. On this basis, susceptibility is the sum of three terms:

$$\chi_{total} = \chi_{organic} + \chi_{anion} + \chi_{tip}$$

The fit from 10−300 K using the model mentioned above for the silicotungstate derivative gives values of $J/k_B$ and $\Delta/k_B$ of −43 K and −145 K, and $\chi_{tip}$ and $C$ are respectively $4.3 \times 10^{-3}$ emu/mol and 0.3446 emu K/mol. It is possible that the Curie susceptibility ascribed to the anion may contain a small contribution due to defects in the BEDT-TTF chains of the type observed in the silicotungstate salt, which would not be deconvoluted by the fitting program.

## Conclusion

Electrocrystallization of BEDT-TTF with α-Keggin anion gives multiple phases with $PMo_{12}O_{40}$ but only one with $SiW_{12}O_{40}$. The crystal structure of $(BEDT\text{-}TTF)_8[PMo_{12}O_{40}]{\cdot}\{(CH_3CN{\cdot}H_2O)_2\}$ is disordered and contains solvent of crystallization. The magnetic properties show nearest-neighbor antiferromagnetic exchange coupling between $(BEDT\text{-}TTF)_2^+$ dimers. Both salts are *Mott−Hubbard insulators* with poor π-electron delocalization between $(BEDT\text{-}TTF^{+1/2})_2$.

**Acknowledgment.** This work was supported by the Progetto Finalizzato *Nuovi Materiali per Tecnologie Avanzate* del Consiglio Nazionale delle Ricerche (Italy) and by EPSRC (U.K.). We acknowledge the British Council and the Italian Ministry of Education for the grant supports the Anglo-Italian collaboration and Mr. P. Filaci and C. Veroli for technical assistance.

**Supporting Information Available:** Crystallographic data, commentary on disorder in the crystal structure, additional figures of the crystal structure of $(BEDT\text{-}TTF)_8[PMo_{12}O_{40}]\{(CH_3CN{\cdot}H_2O)_2\}$, single-crystal reflectivity of $(BEDT\text{-}TTF)_8[SiW_{12}O_{40}]$, half-wave potentials of the donors and acceptors, and spectroscopic data (21 pages); observed and calculated structure factors (14 pages). Ordering information is given on any current masthead page.

CM9500061